RAPID COMMUNICATIONS

PHYSICAL REVIEW C VOLUME 36, NUMBER 5 NOVEMBER 1987

Rapid Communications

The Rapid Communications section is intended for the accelerated publication of important new results. Manuscripts submitted to this section are given priority in handling in the editorial office and in production. A Rapid Communication may be no longer than 3½ printed pages and must be accompanied by an abstract. Page proofs are sent to authors, but, because of the rapid publication schedule, publication is not delayed for receipt of corrections unless requested by the author.

Global optical potentials for elastic p + ^{40}Ca scattering using the Dirac equation

E. D. Cooper
Department of Physics, McGill University, Montreal, Quebec, Canada H3A 2T8

B. C. Clark, R. Kozack,* and S. Shim
Department of Physics, The Ohio State University, Columbus, Ohio 43210

S. Hama, J. I. Johansson, and H. S. Sherif
Theoretical Physics Institute, Department of Physics, University of Alberta, Edmonton, Alberta, Canada T6G 2J1

R. L. Mercer
IBM Thomas J. Watson Research Laboratory, Yorktown Heights, New York 10598

B. D. Serot
Department of Physics, Indiana University, Bloomington, Indiana 47405
(Received 1 July 1987)

We present the first global relativistic optical-model treatment of proton-nucleus elastic scattering. Energy-dependent optical potential parameters for the Lorentz vector and scalar potentials of Dirac phenomenology are given. Several different assumptions regarding the optical-model energy dependence are considered. Constraints from relativistic mean-field theory are presented.

The recent rapid development of relativistic treatments of nuclear reactions has increased the need for relativistic optical model potentials for use in relativistic descriptions of reactions such as (e,e'p), (p,p'), (p,2p), (p,πX), or (γ,p). In this work we give the first results of a global fitting approach using the program GRUNT[1] to obtain these potentials. We consider a large body of elastic scattering data at energies above 150 MeV for p + ^{40}Ca. The standard scalar-vector (SV) model of Dirac phenomenology is employed with several different assumptions for the energy dependence of the potential parameters.

The optical potentials used have the form

$$V(E,r) = V_0(E) f_0(E,r) + iW_0(E) g_0(E,r) , \quad (1)$$

$$S(E,r) = V_S(E) f_S(E,r) + iW_S(E) g_S(E,r) , \quad (2)$$

where $f(E,r)$ and $g(E,r)$ are chosen to be symmetrized two-parameter Fermi shapes,[2]

$$f(E,r) \text{ and } g(E,r) = \left[1+\exp\frac{[r-r_0(E)A^{1/3}]}{a(E)}\right]^{-1}\left[1+\exp\frac{-[r+r_0(E)A^{1/3}]}{a(E)}\right]^{-1} . \quad (3)$$

In this work we consider several different assumptions regarding the energy dependence of the potential parameters above 150 MeV. The extension to lower energies will be given separately,[3] as the shape of the imaginary potentials is expected to deviate from a Fermi form. The dependence on mass number will be considered elsewhere.[4]

In our first parametrization we restricted the geometries of the real optical potentials to shapes shown to produce high quality fits at each energy individually.[5,6] These constraints were based on relativistic mean-field calculations. We considered two different ways of determining the parameters for the form factors of Eq. (3). First (case 1), we considered a simple folding model, described in Ref. 5, based on two-body Yukawa potentials for the exchange of scalar (σ) or vector (ω) mesons. In this case the real vector parameters are $r_{0,v}$ = 1.0159 fm and a_v = 0.6678 fm, and the corresponding scalar parameters are $r_{0,s}$ = 1.0098 fm and a_s = 0.6918 fm. Then we used (case 2) two-parameter Fermi fits to relativistic Hartree potentials.[6-8] These parameters are $r_{0,v}$ = 1.0600 fm and a_v = 0.5817 fm for the vector and $r_{0,s}$ = 1.0672 fm and

TABLE I. Global parameters for the scalar and vector optical potentials for the p+^{40}Ca cases 1 and 2 global fits. The real geometries are energy independent and fixed at either the OBEP geometries (case 1) or the relativistic Hartree geometries (case 2) as described in the text. The energy dependence of the real and imaginary strengths as well as the imaginary geometry parameters is quadratic. The form is given in the text in Eqs. (4).

	Case 1			Case 2		
	a	b	c	a	b	c
V_0	0.8894	−0.3765	0.0700	0.6861	−0.1618	−0.0144
W_0	1.1446	0.1406	−0.0924	0.5030	0.3274	0.0739
$r_{0,v}$	1.0842	−0.0090	−0.0032	1.1658	−0.0882	−0.0224
a_0	0.5702	−0.0599	0.0064	0.4861	0.0603	0.0205
V_s	0.9730	−0.2170	0.0109	0.6987	−0.0506	−0.0336
W_s	1.2072	0.2324	−0.2913	0.3212	0.2613	0.0969
$r_{0,s}$	1.0872	−0.0090	0.0070	1.2019	−0.1026	−0.0681
a_s	0.5587	−0.0452	−0.0521	0.4204	0.0926	0.0282

a_s =0.6111 fm for the scalar. The differences between these sets give some measure of the uncertainty in this constraint procedure.[9] All of the energy dependence of the scalar and vector potentials is in the strengths and in the imaginary geometries.

The real scalar and vector strength parameters and the imaginary scalar and vector strengths and geometry parameters were taken to have parabolic energy dependence of the form

$$V_0(E)=300(a_1+b_1E+c_1E^2)\ , \tag{4a}$$

$$W_0(E)=-100(a_2+b_2E+c_2E^2)\ , \tag{4b}$$

$$V_s(E)=-400(a_3+b_3E+c_3E^2)\ , \tag{4c}$$

$$W_s(E)=100(a_4+b_4E+c_4E^2)\ , \tag{4d}$$

where $E=(T_p-400)/400$ with T_p the projectile kinetic energy is the laboratory frame. The imaginary geometry parameters are also parabolic, for example, $r_0=(a+bE+cE^2)$. In these two cases a total of 24 parameters are varied. The data set we have used contains 1600 data points, so this number of parameters is not excessive. The coefficients a, b, and c for the global best fit potentials are given in Table I for both cases 1 and 2.

Next we investigated a more restrictive scenario in which the parameterized geometries were assumed to be energy independent. All energy dependence is imbedded in the strength parameters. This does not imply that the second-order Dirac equation central and spin-orbit (Schrödinger equivalent) optical potential geometries are energy independent, as neither is linear in S and V.[6] To improve the systematic behavior of the imaginary strengths, we took the imaginary scalar potential to be energy independent. This constrains the ratio of vector to scalar strengths and puts all of the energy dependence in the imaginary vector potential. This also insures reasonable behavior of the imaginary potential strengths.

Two assumptions for the energy dependence of the real scalar and vector and imaginary vector strengths were made. First, the energy dependence was taken to be parabolic (case 3) as in Eqs. (4a)–(4c), and second (case 4) it was assumed to be cubic with the addition of a term dE^3 to Eqs. (4a)–(4c). The number of parameters is 18 in the parabolic case and 21 in the cubic case. The parameters are given in Table II. Note that the parameters in the two cases are quite similar. To check the stability of the fitting, we started the cubic fit in a completely different region of parameter space. The fit was recovered with potential parameters differing by less than 0.1%.

In every case the fits to the p+^{40}Ca data at the individual energies of 161, 181.3, 200, 300, 362, 497.5, 613, 797.5, and 1040 MeV were very good.[10] The fits produced calculated observables for the various cases that are, in general, graphically indistinguishable even though the chi squares per degree of freedom of 15, 22, 17, and 16 for cases 1 through 4 are rather different. Although the fits are of comparable quality, the individual potential parameters at a given energy can be quite different. These differences are most pronounced at the lower energies, for

TABLE II. Global parameters for the scalar and vector optical potentials for p+^{40}Ca for cases 3 and 4. The imaginary scalar potential strength was found to be 66.6224 MeV for case 3 and 64.7099 MeV for case 4.

Case		a	b	c	d
3	V_0	0.8299	−0.1820	−0.0510	· · ·
3	W_0	0.8150	0.0610	0.0290	· · ·
3	V_s	0.8940	−0.0510	−0.0910	· · ·
4	V_0	0.8348	−0.1558	−0.0742	−0.0095
4	W_0	0.8005	0.0711	0.0369	−0.0160
4	V_s	0.8962	−0.0101	−0.0915	−0.0479

Real

Case	$r_{0,v}$ (fm)	a_v (fm)	$r_{0,s}$ (fm)	a_s (fm)
3	1.0137	0.6500	1.0097	0.6866
4	1.0128	0.6485	1.0084	0.6861

Imaginary

Case	$r_{0,v}$ (fm)	a_v (fm)	$r_{0,s}$ (fm)	a_s (fm)
3	1.0792	0.5440	1.0909	0.5053
4	1.0800	0.5443	1.0910	0.5050

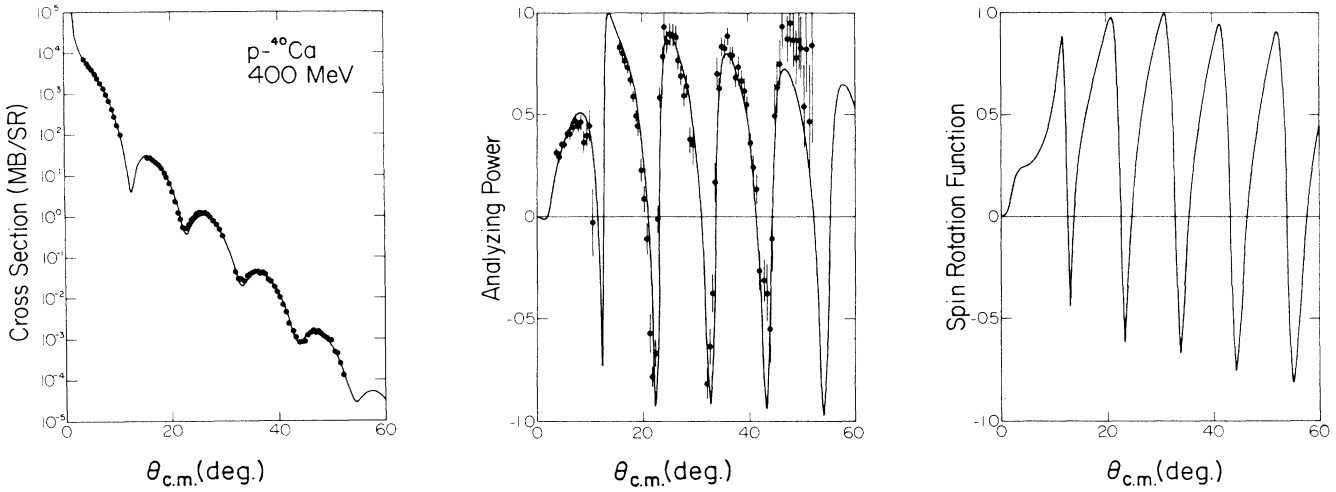

FIG. 1. Predicted elastic observables for p+ ^{40}Ca at 400 MeV. The potentials of case 1 were used in the calculation.

example, at 160 MeV the real vector potential strength varies between 342 MeV (case 1) and 233 MeV (case 2). These differences are due to the strong correlations between individual potential parameters which exist in Dirac optical model fits. Sensitivity of reaction calculations to input optical potentials may be checked by repeating the calculations using potentials corresponding to several different cases. The predictive power of these global fits was tested by predicting observables for an energy not included in the fit. Data at 400 MeV were not included, and the predicted fit for case 1 shown in Fig. 1 is quite acceptable. All cases predict the 400 MeV observables essentially as well; the calculated observables are almost indistinguishable on a graph. Extrapolation to lower or higher energies, is, in general, not advisable for global fits. This is especially true for polynomial parametrizations. We find, for example, that extrapolation to 135 MeV produces very poor agreement with experiment. As mentioned above, work is underway to include mass-number dependence of the potential parameters as well as to extend the range of validity of the parametrizations.[3,4]

We acknowledge the support of the U.S. National Science Foundation, the U.S. Department of Energy, and the National Sciences and Engineering Research Council of Canada.

*Present address: Group T-2 MSB-243, Los Alamos National Laboratory, Los Alamos, NM 87545.

[1]E. D. Cooper, Ph.D thesis, University of Alberta, 1981 (unpublished).

[2]A. M. Kobos, E. D. Cooper, J. I. Johansson, and H. S. Sherif, Nucl. Phys. **A445**, 605 (1985).

[3]E. D. Cooper, B. C. Clark, R. Kozack, S. Shim, S. Hama, H. S. Sherif, and R. L. Mercer, Ohio State University Report No. 170, 1987 (unpublished).

[4]E. D. Cooper, B. C. Clark, R. Kozack, S. Shim, S. Hama, H. S. Sherif, and R. L. Mercer, Ohio State University Report No. 205, 1987 (unpublished).

[5]L. G. Arnold, B. C. Clark, R. L. Mercer, and P. Schwandt, Phys. Rev. C **23**, 1949 (1981).

[6]B. C. Clark, S. Hama, and R. L. Mercer, in *The Interactions Between Medium Energy Nuclei—1982,* edited by H. O. Meyer, AIP Conf. Proc. No. 97 (AIP, New York, 1983), p. 260.

[7]S. Hama, B. C. Clark, R. E. Kozack, S. Shim, E. D. Cooper, R. L. Mercer, and B. D. Serot, Ohio State University Report No. 353, 1987 (unpublished).

[8]C. J. Horowitz and B. D. Serot, Nucl. Phys. **A368**, 503 (1981).

[9]We note that a three-parameter Fermi fit to the relativistic Hartree potentials gave less satisfactory results even though it was a better representation of the relativistic Hartree potentials. Using the relativistic Hartree potentials point-by-point was better than the three-parameter fit but worse than the two-parameter fit.

[10]For references to all of the data except 362 MeV, see P. Schwandt, in *The Interactions Between Medium Energy Nuclei—1982,* edited by H. O. Meyer, AIP Conf. Proc. No. 97 (AIP, New York, 1983), p. 29; the reference for the 362 MeV data is D. Frekers *et al.*, Phys. Rev. C **35**, 2236 (1987).